

Parameter Identification for an Uncooperative Captured Satellite with Spinning Reaction Wheels

Olga-Orsalia Christidi-Loumpasefski, *Student Member, IEEE*
and Evangelos Papadopoulos, *Fellow, IEEE*

Abstract— A novel identification method is developed which identifies the accumulated angular momentum (AAM) of spinning reaction wheels (RWs) of an uncooperative satellite captured by a robotic servicer. In contrast to other methods that treat captured satellite's RWs as non-spinning, the developed method provides simultaneously accurate estimates of the AAM of the captured satellite's RWs and of the inertial parameters of the entire system consisting of the robotic servicer and of the captured satellite. These estimates render the system free-floating dynamics fully identified and available to model-based control. Three-dimensional simulations demonstrate the method's validity. To show its usefulness, the performance of a model-based controller is evaluated with and without knowledge of the captured satellite's RWs AAM.

I. INTRODUCTION

Successes in space exploration have emphasized the growing importance of On-Orbit Servicing (OOS) in space programs. One of the most promising ways to accomplish OOS activities is to exploit robotic servicers, [1], [2]. Moreover, the large amount of satellites launched over the last decades, has resulted in a great number of space debris endangering the success of current and future missions. Consequently, future OOS missions for refueling and repairing of the defunct satellites, the largest space debris on orbit, have been considered by space agencies of vital importance.

To increase a servicer's life and avoid potentially harmful motions, its reaction wheels (RWs) and thrusters are turned off during servicing. This results in a free-floating operation, i.e. no external forces and torques act on the system. Subsequently, manipulator(s) motions result in motion of the uncontrolled robotic servicer's base, due to dynamic coupling between them. Moreover, since reaction wheels are turned off, any accumulated RW angular momentum remains constant. Then, as the servicer base attitude changes, disturbance torques appear due to the RWs. To accomplish the aforementioned OOS tasks at high accuracy, advanced model-based control strategies must be adopted; these require accurate knowledge of system parameters and momenta [3].

However, very often, the dynamic parameters of a robotic servicer may change on orbit for a number of reasons, such as

fuel consumption and payload deployment. Moreover, defunct satellites (see Figure 1) usually have a non-functional attitude control system (ACS) and hence, their RWs may have accumulated angular momentum (AAM) from previous operations. However, the AAM of the RWs of an uncooperative satellite can be unknown due to lack of communication or to system failures. Therefore, the need for parameter identification methods arises.

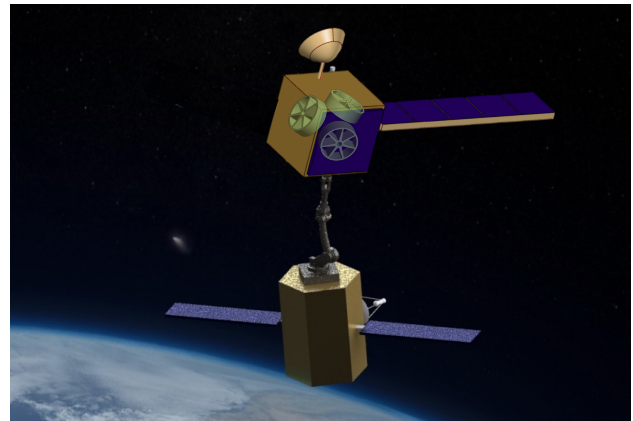


Figure 1. Satellite with rotating RWs captured by a robotic servicer.

A number of researchers have proposed methods to identify the parameters of an unknown satellite in the *pre-capture phase*, while others have developed methods that require the capture phase to be accomplished first. The former are mainly vision-based [4]-[7]. However, vision-based methods can estimate only ratios of the moments of inertia, the location of the center of mass (CM) and the orientation of principal axes.

Most recently developed methods proposed the application of an impulse to the floating satellite and the use of measurements from visual and force sensors, to estimate all satellite inertial parameters [8]-[9]. However, all vision-based algorithms developed so far, do not identify the AAM of satellite RWs; they assume that RWs are not spinning. This is unrealistic for uncooperative defunct satellites and endangers servicing missions.

Nevertheless, methods that assume *prior capture* are very useful too, since potentially they can provide the controller with the mass matrices of the entire robotic servicer, compensating for uncertainties not only of the captured satellite and of the servicer, but also of their connection special characteristics (e.g., exact pickup location). These methods can be classified to those that use the *equations of motion* and those based on *momentum principles*. Examples

Olga-Orsalia Christidi-Loumpasefski was supported by an *Onassis Foundation Scholarship*.

The second author acknowledges partial support by the H2020 Operational Grant n°7 – EROSS, funded by the European Commission under Grant Agreement #821904.

Olga-Orsalia Christidi-Loumpasefski and Evangelos Papadopoulos are with the School of Mechanical Engineering, NTUA, Greece (e-mail: [ol-gachr, egpapado]@central.ntua.gr; phone: +30-210-772-1440).

of the former include [10]-[14]. The main disadvantage of all methods based on the equations of motion, is the requirement for acceleration measurements, which contain substantial noise corrupting the estimates.

To tackle this issue, other researchers have formulated identification methods based on momentum equations, [10], [15]-[18]. Xu et al. proposed a method that uses both equations of motion and momentum equations [19]. However, all such algorithms also treat captured satellite RWs as non-rotating, with the same potential mission risks.

In our previous work, we proposed a momentum-based method that allows identification of all system inertial parameters for free-floating dynamics reconstruction of a robotic servicer with/without a captured satellite [18]. Compared to the ones proposed in the literature, this method is superior as it yields all inertial parameters and has distinct accuracy advantages in the presence of noise. Although this is an important achievement, additional identification of the AMM of the captured satellite RWs is required by model-based advanced controllers.

In this paper, a novel identification method is developed, which in contrast to other methods, provides accurate estimates of both the AAM of the captured satellite RWs and of the inertial parameters of the entire system consisting of the robotic servicer and the captured satellite. These estimates render a system's free-floating dynamics fully identified and applicable to model-based control. The importance of identifying the AAM for control is shown by an example.

II. DYNAMICS OF FREE-FLOATING SPACE MANIPULATORS

In this section, the dynamics of a free-floating robotic servicer (FFRS), which has captured a satellite with initial AAM on its RWs, is presented briefly. Figure 2 shows a FFRS consisting of a spacecraft (SC) equipped with $N_{rs,rw}$ RWs, and with n manipulators or appendages with revolute joints, in an open chain kinematic configuration, which has captured a satellite equipped with $N_{s,rw}$ RWs. The captured satellite is considered as part of the servicer's last link. Also, rigid grasp is assumed; orbital disturbances are neglected.

The m -th manipulator has N_m links, and the sum of all manipulator links K is equal to

$$K = \sum_{m=1}^n N_m \quad (1)$$

A frame $\theta\{x_0, y_0, z_0\}$ is attached at the SC center of mass (CM). A SC *feature point* S is tracked, and an observation frame $b\{x_b, y_b, z_b\}$ is attached to it, with orientation that of frame θ . Moreover, a frame $rs,rw,i\{x_{rs,rw,i}, y_{rs,rw,i}, z_{rs,rw,i}\}$ is attached to robotic servicer's i^{th} RW and a frame $s,rw,i\{x_{s,rw,i}, y_{s,rw,i}, z_{s,rw,i}\}$ is attached to captured satellite's i^{th} RW. Frame $i\{X, Y, Z\}$ is the inertial frame.

In free-floating mode, the system center of mass (CM) remains fixed in inertial space. Thus, the origin of the inertial frame can be chosen to be at the system CM. In free-floating operation, both the servicer's thrusters and RWs are off.

A left superscript on (\bullet) indicates the frame in which (\bullet) is expressed. No left superscript is used for the inertial frame.

A. System Angular Momentum

Due to the importance of the RW angular momentum, the *system* angular momentum with respect to the system CM, \mathbf{h}_{cm} , is written as the sum of the robotic servicer's angular momentum \mathbf{h}_{rs} , its RWs angular momentum due to their relative motion with respect to the servicer SC $\mathbf{h}_{rs,rw/sc}$, and the AAM of the captured satellite's RWs due to their relative motion with respect to the servicer last link $\mathbf{h}_{s,rw/N}$

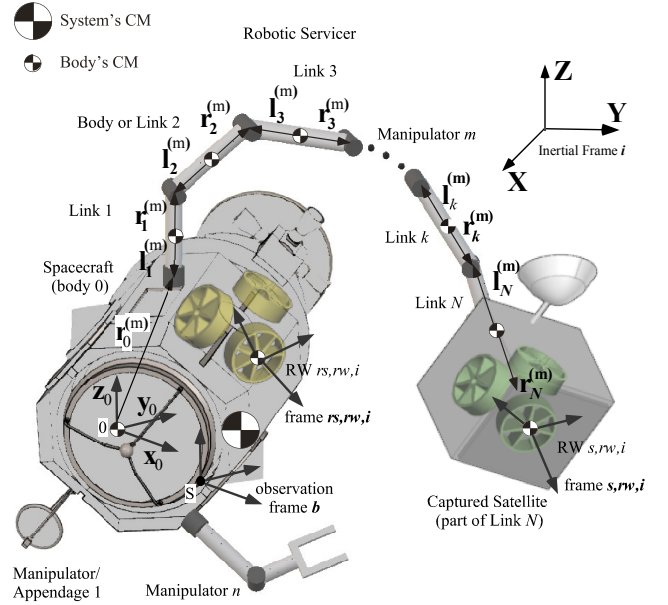


Figure 2. An uncooperative satellite captured by a robotic servicer.

$$\mathbf{h}_{cm} = \mathbf{h}_{rs} + \mathbf{h}_{rs,rw/sc} + \mathbf{h}_{s,rw/N} = const. \quad (2)$$

The robotic servicer angular momentum \mathbf{h}_{rs} is [20]:

$$\mathbf{h}_{rs} = \mathbf{R}_0 ({}^0\mathbf{D}^0 \boldsymbol{\omega}_0 + {}^0\mathbf{D}_q \dot{\mathbf{q}}) \quad (3)$$

where ${}^0\boldsymbol{\omega}_0$ is the SC angular velocity and the column vector $\dot{\mathbf{q}}$ is:

$$\dot{\mathbf{q}} = [\dot{\mathbf{q}}^{(1)T} \quad \dots \quad \dot{\mathbf{q}}^{(m)T} \quad \dots \quad \dot{\mathbf{q}}^{(n)T}]^T \quad (4)$$

where the $N_m \times 1$ column-vector $\dot{\mathbf{q}}^{(m)}$ represents the joint rates vector of the m -th manipulator. The matrix \mathbf{R}_0 is the rotation matrix between the θ frame and the inertial frame, expressed as a function of the Euler parameters $\boldsymbol{\varepsilon}, \boldsymbol{\eta}$. The inertia-type matrices ${}^0\mathbf{D}, {}^0\mathbf{D}_q$ are given in [18] and they include the inertial parameters of the RWs as part of the SC inertial parameters.

The angular momentum of the robotic servicer's RWs due to their relative motion with respect to the servicer SC, $\mathbf{h}_{rs,rw/sc}$, is given by:

$$\mathbf{h}_{rs,rw/sc} = \mathbf{R}_0 {}^0\mathbf{h}_{rs,rw/sc} = \mathbf{R}_0 {}^0\mathbf{D}_{rs,rw} \dot{\mathbf{q}}_{rs,rw} = \mathbf{D}_{rs,rw} \dot{\mathbf{q}}_{rs,rw} \quad (5)$$

where $\dot{\mathbf{q}}_{rs,rw}$ is the column vector of the robotic servicer's RW relative angular rates, and the inertia-type matrix ${}^0\mathbf{D}_{rs,rw}$ is given by:

$${}^0\mathbf{D}_{rs,rw} = \begin{bmatrix} {}^0\mathbf{D}_{rs,rw,1} & \dots & {}^0\mathbf{D}_{rs,rw,N_{rs,rw}} \end{bmatrix} \quad (6)$$

where

$${}^0\mathbf{D}_{rs,rw,i} = {}^0\mathbf{R}_{rs,rw,i} {}^{rs,rw,i}\mathbf{I}_{rs,rw,i} {}^{rs,rw,i}\hat{\mathbf{z}}_{rs,rw,i} \quad i = 1, \dots, N_{rs,rw} \quad (7)$$

and ${}^{rs,rw,i}\mathbf{I}_{rs,rw,i}$ is the robotic servicer's i^{th} RW's moment of inertia, ${}^0\mathbf{R}_{rs,rw,i}$ is the rotation matrix between the rs,rw,i frame and the θ frame and thus it is constant over time, and ${}^{rs,rw,i}\hat{\mathbf{z}}_{rs,rw,i}$ is the unit vector along the robotic servicer's i^{th} RW rotation axis.

The AAM of the captured satellite's RWs due to their relative motion with respect to the servicer last link $\mathbf{h}_{s,rw/N}$ is given by:

$$\mathbf{h}_{s,rw/N} = \mathbf{R}_0 {}^0\mathbf{R}_N {}^N\mathbf{h}_{s,rw/N} = \mathbf{R}_0 {}^0\mathbf{R}_N {}^N\mathbf{D}_{s,rw} \dot{\mathbf{q}}_{s,rw} \quad (8)$$

where ${}^0\mathbf{R}_N$ is the rotation matrix between the body-fixed (N) frame of link N and the θ frame, $\dot{\mathbf{q}}_{s,rw}$ is the column vector of the captured satellite's RW relative angular rates, and the inertia-type matrix ${}^N\mathbf{D}_{s,rw}$ is given by:

$${}^N\mathbf{D}_{s,rw} = \begin{bmatrix} {}^N\mathbf{D}_{s,rw,1} & \dots & {}^N\mathbf{D}_{s,rw,N_{s,rw}} \end{bmatrix} \quad (9)$$

where

$${}^N\mathbf{D}_{s,rw,i} = {}^N\mathbf{R}_{s,rw,i} {}^{s,rw,i}\mathbf{I}_{s,rw,i} {}^{s,rw,i}\hat{\mathbf{z}}_{s,rw,i} \quad i = 1, \dots, N_{s,rw} \quad (10)$$

where ${}^{s,rw,i}\mathbf{I}_{s,rw,i}$ is the captured satellite's i^{th} RW's moment of inertia, ${}^N\mathbf{R}_{s,rw,i}$ is the rotation matrix between the s,rw,i frame and the θ frame and thus it is constant over time, and ${}^{s,rw,i}\hat{\mathbf{z}}_{s,rw,i}$ is the unit vector along the captured satellite's i^{th} RW rotation axis. The captured satellite's RWs joint rates remain constant as no torques are applied to the RWs of an uncooperative satellite.

An important remark here is that \mathbf{h}_{cm} remains constant when the system is in free-floating mode, i.e no external forces and moments act on it. Moreover, ${}^0\mathbf{h}_{rs,rw/sc}$ is known since the robotic servicer's RWs inertias are assumed to be known, and remains constant since they are not actuated. Therefore, solving for \mathbf{h}_{cm} yields:

$$\mathbf{h}_{rs} = -\mathbf{R}_0 {}^0\mathbf{h}_{rs,rw/sc} - \mathbf{R}_0 {}^0\mathbf{R}_N {}^N\mathbf{h}_{s,rw/N} + \mathbf{h}_{cm} \quad (11)$$

By differentiating (11), the system dynamic equations are obtained:

$${}^0\mathbf{D}(\mathbf{q}) {}^0\dot{\boldsymbol{\omega}}_0 + {}^0\mathbf{D}_q(\mathbf{q})\dot{\mathbf{q}} + \mathbf{c}_1({}^0\boldsymbol{\omega}_0, \mathbf{q}, \dot{\mathbf{q}}) = \mathbf{R}_0^T \mathbf{g}_{cm} \quad (12)$$

where

$$\mathbf{g}_{cm} = -\mathbf{R}_0 {}^0\boldsymbol{\omega}_0 \times {}^0\mathbf{h}_{rs,rw/sc} - \mathbf{R}_0 {}^0\mathbf{R}_N {}^N\boldsymbol{\omega}_N \times {}^N\mathbf{h}_{s,rw/N} \quad (13)$$

and $(*)^\times$ is the cross-product matrix of vector $(*)$.

The angular velocity of link N ${}^N\boldsymbol{\omega}_N$ is given by [20]:

$${}^N\boldsymbol{\omega}_N = \mathbf{R}_0^T {}^0\mathbf{R}_N^T \boldsymbol{\omega}_N = \mathbf{R}_0^T {}^0\mathbf{R}_N^T \mathbf{R}_0 \left({}^0\boldsymbol{\omega}_0 + \sum_{k=1}^N {}^0\mathbf{F}_k \dot{\mathbf{q}} \right) \quad (14)$$

where

$${}^0\mathbf{F}_k = [{}^0\mathbf{R}_1 {}^1\hat{\mathbf{z}}_1 \quad \dots \quad {}^0\mathbf{R}_k {}^k\hat{\mathbf{z}}_k \quad \mathbf{0}_{3 \times (K-k)}] \quad (15)$$

where ${}^0\mathbf{R}_k$ is the rotation matrix between the body-fixed (k) frame of link k and the θ frame and ${}^k\hat{\mathbf{z}}_k$ is the unit vector along the robotic servicer's k^{th} joint's rotation axis.

The left side of the equations of motion (12) for the servicer is derived in [21]; however in [21] there are no rotating RWs and therefore no disturbances act on the SC or

the last link, i.e. $\mathbf{g}_{cm} = \mathbf{0}$. The reduced equations of motion of the free-floating servicer are [21]:

$${}^0\mathbf{D}_q^T(\mathbf{q}) {}^0\dot{\boldsymbol{\omega}}_0 + {}^0\mathbf{D}_{qq}(\mathbf{q})\dot{\mathbf{q}} + \mathbf{c}_2({}^0\boldsymbol{\omega}_0, \mathbf{q}, \dot{\mathbf{q}}) = \boldsymbol{\tau} \quad (16)$$

where the inertia-type matrices ${}^0\mathbf{D}$, ${}^0\mathbf{D}_q$, ${}^0\mathbf{D}_{qq}$ are as in [18] and the column vectors \mathbf{c}_1 , \mathbf{c}_2 are as in [22], and $\boldsymbol{\tau}$ is the vector of the manipulator joint torques.

Since ${}^0\mathbf{D}$ is always invertible, solving (12) for ${}^0\dot{\boldsymbol{\omega}}_0$ and substituting in (16) yields:

$${}^0\mathbf{D}_{qq}\dot{\mathbf{q}} - {}^0\mathbf{D}_q^T {}^0\mathbf{D}^{-1} {}^0\mathbf{D}_q\dot{\mathbf{q}} + \mathbf{c}_2 - {}^0\mathbf{D}_q^T {}^0\mathbf{D}^{-1} (\mathbf{c}_1 - \mathbf{R}_0^T \mathbf{g}_{cm}) = \boldsymbol{\tau} \quad (17)$$

or, equivalently

$$\mathbf{H}(\mathbf{q})\dot{\mathbf{q}} + \mathbf{c}({}^0\boldsymbol{\omega}_0, \mathbf{q}, \dot{\mathbf{q}}, \boldsymbol{\varepsilon}, \boldsymbol{\eta}, {}^0\mathbf{h}_{rs,rw/sc}, {}^N\mathbf{h}_{s,rw/N}) = \boldsymbol{\tau} \quad (18)$$

where

$$\mathbf{H}(\mathbf{q}) = {}^0\mathbf{D}_{qq} - {}^0\mathbf{D}_q^T {}^0\mathbf{D}^{-1} {}^0\mathbf{D}_q \quad (19)$$

$$\mathbf{c} = \mathbf{c}_2 - {}^0\mathbf{D}_q^T {}^0\mathbf{D}^{-1} (\mathbf{c}_1 - \mathbf{R}_0^T \mathbf{g}_{cm}) \quad (20)$$

III. PARAMETER IDENTIFICATION METHOD

To use (2) for parameter identification, the robotic servicer's angular momentum \mathbf{h}_{rs} must be expressed linearly with respect to a parameter vector $\boldsymbol{\pi}$. This procedure is described in detail in [18]. Thus, the servicer angular momentum is written as:

$$\mathbf{h}_{rs} = \mathbf{Y}(\dot{\mathbf{q}}, \mathbf{q}, \boldsymbol{\omega}_0, \boldsymbol{\varepsilon}, \boldsymbol{\eta}) \boldsymbol{\pi} \quad (21)$$

where the $3 \times k$ matrix \mathbf{Y} is the regressor matrix and k is the dimension of $\boldsymbol{\pi}$. The key feature of this regressor is that in contrast to other methods, it does *not* require noisy acceleration measurements. Hence, the system angular momentum \mathbf{h}_{cm} (see Eq. (2)) can be written as:

$$\mathbf{h}_{cm} = \mathbf{Y}\boldsymbol{\pi} + \mathbf{R}_0 {}^0\mathbf{h}_{rs,rw/sc} + \mathbf{R}_0 {}^0\mathbf{R}_N {}^N\mathbf{h}_{s,rw/N} \quad (22)$$

To solve (22) for $\boldsymbol{\pi}$ and the AAM of the captured satellite's RWs ${}^N\mathbf{h}_{s,rw/N}$, \mathbf{h}_{cm} must be known. Since \mathbf{h}_{cm} remains constant:

$$\mathbf{h}_{cm} = (\mathbf{h}_{cm})_{in} \quad (23)$$

where $(*)_{in}$ is the initial value of $(*)$. Hence, applying (2) yields

$$(\mathbf{h}_{cm})_{in} = (\mathbf{h}_{rs})_{in} + (\mathbf{h}_{rs,rw/sc})_{in} + (\mathbf{h}_{s,rw/N})_{in} \quad (24)$$

and subsequently

$$(\mathbf{h}_{cm})_{in} = \mathbf{Y}_{in} \boldsymbol{\pi} + (\mathbf{R}_0)_{in} {}^0\mathbf{h}_{rs,rw/sc} + (\mathbf{R}_0)_{in} ({}^N\mathbf{R}_0)_{in} {}^N\mathbf{h}_{s,rw/N} \quad (25)$$

where ${}^0\mathbf{h}_{rs,rw/sc}$ is also constant since no RW torques are applied during the identification. Thus, (23) and (25) provide the required \mathbf{h}_{cm} .

Assuming N measurements of the variables $(\dot{\mathbf{q}}, \mathbf{q}, \boldsymbol{\omega}_0)$, and $\boldsymbol{\varepsilon}$, $\boldsymbol{\eta}$ are obtained at time instants t_1, t_2, \dots, t_N during the task, Eqs. (22)-(25) result in the following system of equations

$$\hat{\mathbf{b}} = \begin{bmatrix} \mathbf{b}(t_1) \\ \mathbf{b}(t_2) \\ \vdots \\ \mathbf{b}(t_N) \end{bmatrix} = \begin{bmatrix} \mathbf{A}(t_1) \\ \mathbf{A}(t_2) \\ \vdots \\ \mathbf{A}(t_N) \end{bmatrix} \mathbf{x} = \hat{\mathbf{A}}\mathbf{x} \quad (26)$$

where

$$\mathbf{A}(t) = \begin{bmatrix} \mathbf{R}_0(t)^0 \mathbf{R}_N(t) - (\mathbf{R}_0)_{in} ({}^0 \mathbf{R}_N)_{in} & \mathbf{Y}(t) - \mathbf{Y}_{in} \end{bmatrix} \quad (27)$$

$$\mathbf{b}(t) = ((\mathbf{R}_0)_{in} - \mathbf{R}_0(t))^0 \mathbf{h}_{rs,rw/sc} \quad (28)$$

$$\mathbf{x} = \begin{bmatrix} N \mathbf{h}_{s,rw/N} \\ \boldsymbol{\pi} \end{bmatrix}_{(3+k) \times 1} \quad (29)$$

In case the robotic servicer is initially at rest and only its RWs have accumulated angular momentum, a realistic scenario after a stabilization procedure, (26) still holds with $(\mathbf{Y})_{in} = \mathbf{0}$. In case both robotic servicer and its RWs are initially at rest, hence $(\mathbf{h}_{cm})_{in} = (\mathbf{h}_{s,rw/N})_{in}$, angular momentum must be introduced in the RWs. This can be implemented by setting desired RWs joint rates $(\dot{\mathbf{q}}_{rs,rw})_{des}$ and employing a velocity controller. After the torque application of the SC RWs, they are turned off left to spin with the desired accumulated angular momentum:

$$({}^0 \mathbf{h}_{rs,rw/sc})_{des} = {}^0 \mathbf{D}_{rs,rw} (\dot{\mathbf{q}}_{rs,rw})_{des} \quad (30)$$

In this case, (27) becomes:

$$\mathbf{A}(t) = \begin{bmatrix} \mathbf{R}_0(t)^0 \mathbf{R}_N(t) - (\mathbf{R}_0)_{in} ({}^0 \mathbf{R}_N)_{in} & \mathbf{Y}(t) \end{bmatrix} \quad (31)$$

$$\mathbf{b}(t) = -\mathbf{R}_0(t) ({}^0 \mathbf{h}_{rs,rw/sc})_{des} \quad (32)$$

The estimated regressor matrix $\hat{\mathbf{A}}$ must be of full rank for (26) to be solved for \mathbf{x} , which in turn requires $\boldsymbol{\pi}$ to be a minimal parameter set, obtained as in [18]. To ensure that $\hat{\mathbf{A}}$ is of full rank and with a small condition number, the joint exciting trajectories are based on truncated Fourier series with a fifth-order polynomial also added, [18]

$$q_i^{(m)} = \sum_{l=1}^{N_f} \frac{a_l^{i(m)}}{\omega_f l} \sin(\omega_f l t) - \frac{b_l^{i(m)}}{\omega_f l} \cos(\omega_f l t) + \sum_{j=0}^5 c_j^{i(m)} t^j \quad (33)$$

where $m = 1, \dots, n$, $i = 1, \dots, N_m$, N_f is the number of the harmonics employed, $\omega_f = 2\pi/t_f$ with t_f the motion duration, and $a_l^{i(m)}$ and $b_l^{i(m)}$ the free coefficients obtained by minimizing the condition number of the regressor matrix.

Measurement of robotic servicer's RWs joint rates is required also. Measurements of RWs joint rates during the joint trajectories are not required since they remain constant. Nevertheless, all required quantities can be obtained directly or indirectly by available sensors. The required joint angles \mathbf{q} are obtained directly by the joint motor encoders, while their differentiation provides the joint rates $\dot{\mathbf{q}}$. RW rates $\dot{\mathbf{q}}_{rs,rw}$ are obtained by differentiating $\mathbf{q}_{rs,rw}$, obtained directly from the corresponding encoders. The orientation of the servicer base, and thus the corresponding Euler parameters $\boldsymbol{\varepsilon}$, $\boldsymbol{\eta}$, are obtained directly using star or sun trackers, while $\boldsymbol{\omega}_0$ is provided by on board IMUs.

The system of equations given by (26), is over-determined and either recursive or non-recursive methods (e.g. least squares) can be used for solving it (not in the scope of this work).

IV. SIMULATION RESULTS

A. Identification Results

The proposed identification method is illustrated by a spatial robotic servicer with a 3-DOF manipulator. The kinematic and dynamic parameters of the servicer are given in Table I. The joint-space minimal set of parameters of the simulated servicer, i.e. the elements of vector $\boldsymbol{\pi}$, are as in [18].

The robotic servicer's RWs angular momentum due to their relative motion with respect to the servicer SC is ${}^0 \mathbf{h}_{rs,rw/sc} = [25 \ 27 \ 28]^T Nms$ and the AAM of the captured satellite's RWs due to their relative motion with respect to the servicer last link is ${}^N \mathbf{h}_{s,rw/N} = [42 \ 49 \ 41]^T Nms$. The initial base attitude is $[\boldsymbol{\varepsilon}_{in}^T, \boldsymbol{\eta}_{in}^T]^T = [0.2 \ 0.1 \ 0.3 \ 0.927]^T$. The initial joint angles are $\mathbf{q}_{in} = [0 \ 0 \ 0]^T rad$. The SC initial angular velocity is ${}^0 \boldsymbol{\omega}_0 = [0.1 \ 0.12 \ 0.08]^T rad/s$. The joints are initially at rest.

TABLE I. PARAMETERS OF THE SYSTEM UNDER STUDY.

i	l_i (m)	r_i (m)	m_i (kg)	I_{xx} (kg m ²)	I_{yy} (kg m ²)	I_{zz} (kg m ²)
0	-	[0.5,0.5,1] ^T	2000	1500	1500	1500
1	0.25	0.25	50	0.1	11	11
2	1.0	1.0	100	0.1	33	33
3	1.0	1.0	500	400	300	350

In this simulation, $t_f = 20$ s and $N_f = 3$. The desired initial and final conditions correspond to zero joint angles, rates and accelerations. The desired joint trajectory is described by the functions $\mathbf{q}_d(t)$, $\dot{\mathbf{q}}_d(t)$, $\ddot{\mathbf{q}}_d(t)$ based on (33). The coefficients a_l^i and b_l^i of the optimized exciting joint trajectories for minimum condition number of the regressor matrix, are derived for this simulation study and presented in Table II. The number of measurements is $N = 1000$ and the sampling rate is 50 ms.

TABLE II. OPTIMIZED TRAJECTORY COEFFICIENTS.

a_1^1	0.1234	a_2^1	-0.1867	a_3^1	0.0005
a_1^2	0.1306	a_2^2	-0.1222	a_3^2	-0.3760
a_1^3	0.15486	a_2^3	-0.1269	a_3^3	0.4030
b_1^1	0.1600	b_2^1	-0.3808	b_3^1	0.0513
b_1^2	-0.1179	b_2^2	0.1787	b_3^2	-0.1333
b_1^3	-0.0458	b_2^3	0.1346	b_3^3	0.1389

In Figure 3, the joint torques required for the joint trajectories (a) and the SC angular velocity, (b), respectively, during the identification, are shown.

Using a least squares solution of (26), the parameter vector \mathbf{x} is identified without noise and in the presence of noise. The relative errors (RE) of the identified parameters are shown in TABLE III. The noise models used are described in detail in [18]. Hence, the proposed method estimates both the AAM of the captured satellite RWs and the inertial parameters of the entire system consisting of the robotic servicer and the

captured satellite, practically exactly. These parameters are enough to reconstruct the system's free-floating dynamics.

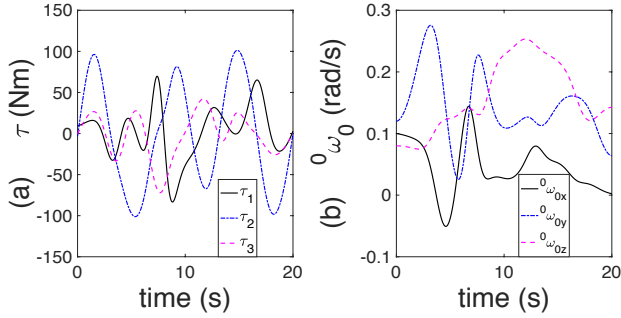


Figure 3. Manipulator joint torques (a) and SC angular velocity (b).

TABLE III. SIMULATION IDENTIFICATION OF PARAMETER VECTOR \mathbf{x} .

	RE (%)	RE (%) + noise		RE (%)	RE (%) + noise
x_1	6e-11	0.16	x_{13}	3e-11	0.14
x_2	-4e-10	-0.96	x_{14}	7e-11	0.14
x_3	-2e-10	-0.75	x_{15}	7e-11	0.17
x_4	6e-11	0.17	x_{16}	1e-10	0.17
x_5	1e-10	0.12	x_{17}	-9e-12	0.09
x_6	6e-11	0.16	x_{18}	6e-11	0.13
x_7	4e-11	0.10	x_{18}	3e-10	0.46
x_8	6e-11	0.16	x_{19}	6e-11	0.17
x_9	6e-11	0.17	x_{20}	7e-11	0.17
x_{10}	6e-11	0.17	x_{21}	6e-11	0.16
x_{12}	4e-11	0.15	x_{21}	6e-11	0.16

B. Importance of RWs AAM Knowledge for Control

To demonstrate the importance of identifying the captured satellite RWs AAM, two controllers are used for the same desired joint trajectory and with the same gains; the first controller (CWK) has knowledge of the AAM of the captured satellite RWs while the second controller (CNK) does not. The desired joint trajectory are described by the functions $\mathbf{q}_d(t), \dot{\mathbf{q}}_d(t), \ddot{\mathbf{q}}_d(t)$ based on (33). The coefficients a_i^j and b_i^j are presented in Table II.

The model-based CWK law is given by:

$$\boldsymbol{\tau} = \mathbf{H}(\ddot{\mathbf{q}}_d + \mathbf{K}_d \dot{\mathbf{e}} + \mathbf{K}_p \mathbf{e}) + \mathbf{c} \quad (34)$$

where \mathbf{e} is the joint position error, and vector \mathbf{c} is given by (20), and hence it contains both terms due to the servicer's RWs relative angular momentum with respect to the SC, i.e. the term $-\mathbf{R}_0^0 \boldsymbol{\omega}_0^{\times 0} \mathbf{h}_{rs,rw/sc}$ in \mathbf{g}_{cm} , and to the AAM of the captured satellite's RWs, i.e. the term $-\mathbf{R}_0^0 \mathbf{R}_N^N \boldsymbol{\omega}_N^{\times N} \mathbf{h}_{s,rw/N}$ in \mathbf{g}_{cm} .

Substituting \mathbf{c} (see (20)) and \mathbf{g}_{cm} (see (13)), (34) can be written further:

$$\boldsymbol{\tau} = \mathbf{H}(\ddot{\mathbf{q}}_d + \mathbf{K}_d \dot{\mathbf{e}} + \mathbf{K}_p \mathbf{e}) + \mathbf{c}_2 - {}^0\mathbf{D}_q^T \mathbf{D}^{-1} (\mathbf{c}_1 + {}^0\boldsymbol{\omega}_0^{\times 0} \mathbf{h}_{rs,rw/sc} + {}^0\mathbf{R}_N^N \boldsymbol{\omega}_N^{\times N} \mathbf{h}_{s,rw/N}) \quad (35)$$

The application of (34) on the system equations of motion

(18) results in the following error dynamics,

$$\ddot{\mathbf{e}} + \mathbf{K}_d \dot{\mathbf{e}} + \mathbf{K}_p \mathbf{e} = \mathbf{0} \quad (36)$$

in which the selection of appropriate positive definite gain matrices $\mathbf{K}_p, \mathbf{K}_d$ ensures the stability of the dynamics and zero steady state joint error in desired time.

On the contrary, the model-based CNK law is given by:

$$\boldsymbol{\tau} = \mathbf{H}(\mathbf{q})(\ddot{\mathbf{q}}_d + \mathbf{K}_d \dot{\mathbf{e}} + \mathbf{K}_p \mathbf{e}) + \mathbf{c}_2 - {}^0\mathbf{D}_q^T \mathbf{D}^{-1} (\mathbf{c}_1 + {}^0\boldsymbol{\omega}_0^{\times 0} \mathbf{h}_{rs,rw/sc}) \quad (37)$$

Note that this law contains only the term caused by servicer's RWs relative angular momentum with respect to the SC, i.e. the term $-\mathbf{R}_0^0 \boldsymbol{\omega}_0^{\times 0} \mathbf{h}_{rs,rw/sc}$ in \mathbf{g}_{cm} , and not the term caused by the AAM of the captured satellite's RWs, i.e. the term $-\mathbf{R}_0^0 \mathbf{R}_N^N \boldsymbol{\omega}_N^{\times N} \mathbf{h}_{s,rw/N}$ in \mathbf{g}_{cm} .

The application of (37) on the system equations of motion (18) results in the following error dynamics:

$$\ddot{\mathbf{e}} + \mathbf{K}_d \dot{\mathbf{e}} + \mathbf{K}_p \mathbf{e} = -\mathbf{H}^{-1} ({}^0\mathbf{D}_q^T \mathbf{D}^{-1} {}^0\mathbf{R}_N^N \boldsymbol{\omega}_N^{\times N} \mathbf{h}_{s,rw/N}) = \mathbf{a} \quad (38)$$

The RHS of (38), i.e. \mathbf{a} , is function of $\mathbf{q}, \dot{\mathbf{q}}, \boldsymbol{\varepsilon}, \boldsymbol{\eta}, {}^0\boldsymbol{\omega}_0, {}^N\mathbf{h}_{s,rw/N}$ since matrices $\mathbf{H}, {}^0\mathbf{D}_q, {}^0\mathbf{D}, {}^0\mathbf{R}_N$ are functions of \mathbf{q} and vector ${}^N\boldsymbol{\omega}_N$ (see (14)) is function of $\mathbf{q}, \dot{\mathbf{q}}, \boldsymbol{\varepsilon}, \boldsymbol{\eta}, {}^0\boldsymbol{\omega}_0$. Hence, applying this control law and assuming existence of a steady state error \mathbf{e}_{ss} ($\mathbf{q} = \mathbf{q}_{ss}, \dot{\mathbf{q}} = \mathbf{0}, \ddot{\mathbf{e}} = \mathbf{0}$) yields the following:

$$\mathbf{e}_{ss} = \mathbf{K}_p^{-1} \mathbf{a}(\mathbf{q}_{ss}, \boldsymbol{\varepsilon}, \boldsymbol{\eta}, {}^0\boldsymbol{\omega}_0, {}^N\mathbf{h}_{s,rw/N}) \quad (39)$$

However, \mathbf{e}_{ss} is a function of $\boldsymbol{\varepsilon}, \boldsymbol{\eta}$ and ${}^0\boldsymbol{\omega}_0$ which vary with time. Hence, in this case the error cannot converge to zero.

Figures 4 and 5 show the joint torques (a) and the SC angular velocity (b) for the CWK and CNK, respectively. Observing Figure 6 and comparing the absolute errors for the CWK (a) and CNK (b) one can see that knowing the captured satellite RWs AAM results in significant improvement on the joint trajectories errors. In practice, errors will be larger than those presented here due to sensor noise and unmodelled uncertainties; however, the identification still will be necessary as it results in vastly improved trajectory tracking.

As shown in Figure 6, and in contrast to CWK, the CNK maximum absolute joint position error is almost 8 degrees, which corresponds in 90 cm of maximum end-effector position error, see Figure 7; this is unacceptable for servicing missions.

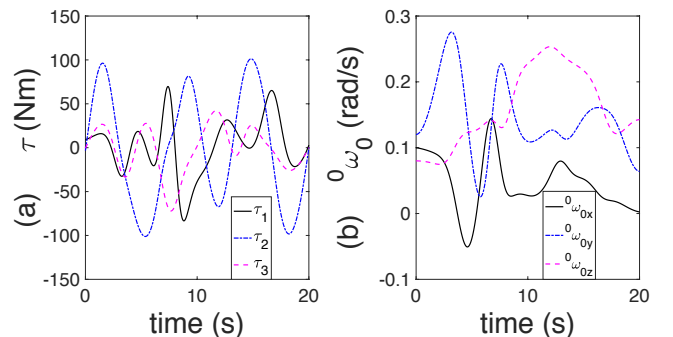


Figure 4. (a) Joint torques and (b) SC angular velocity with CWK.

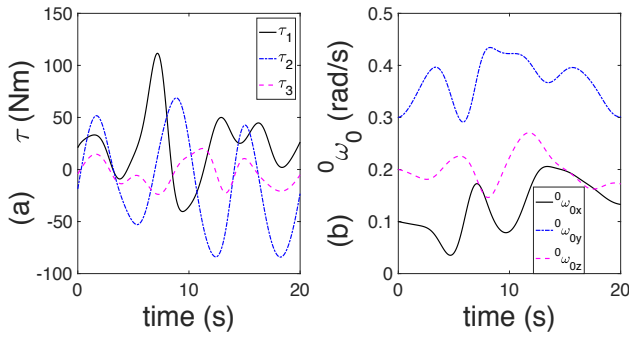


Figure 5. (a) Joint torques and (b) SC angular velocity CNK.

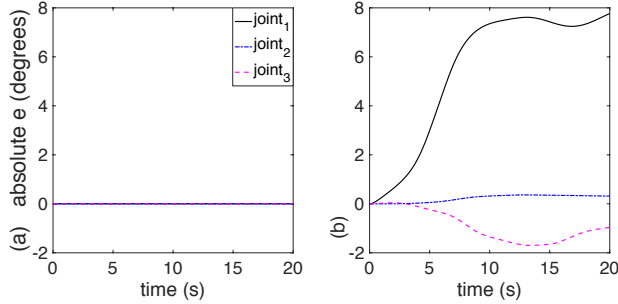


Figure 6. Absolute joint position errors due to the CWK (a) and due to the CNK (b).

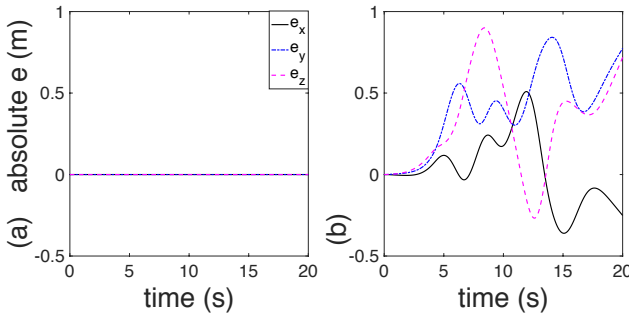


Figure 7. Absolute end-effector position error due to the CWK (a) and due to the CNK (b).

V. CONCLUSION

In this paper, an identification method is developed which, in contrast to other methods which treat captured satellite's RWs as non-spinning, provides simultaneously accurate estimates of the AAM of the captured satellite's RWs and of the inertial parameters of the entire system consisting of the robotic servicer and the captured satellite. These estimates render system free-floating dynamics fully identified and applicable to advanced model-based control strategies during on-orbit servicing tasks. Three-dimensional simulations demonstrate the method's validity. To show the necessity of the proposed method, the manipulator tracking performance using a model-based controller with and without knowledge of AAM of the captured satellite's RWs was evaluated. Results show that identification of the AAM of the captured satellite allows vastly improved trajectory tracking.

REFERENCES

[1] Oda, M., "Space robot experiments on NASDA's ETS-VII satellite-preliminary overview of the experiment results," *IEEE International*

Conference on Robotics and Automation (ICRA '99), Detroit, Michigan, USA, May 1999, pp. 1390-1395.

[2] Ogilvie, A., Allport, J., Hannah, M., and Lymer, J., "Autonomous Satellite Servicing Using the Orbital Express Demonstration Manipulator System," *International Symposium on Artificial Intelligence, Robotics and Automation in Space, (i-SAIRAS '08)*, February 26 - 29, 2008, Hollywood, USA.

[3] Moosavian, S. Ali A. and Papadopoulos, E. "Multiple Impedance Control for Object Manipulation," *IEEE/RSJ Intl. Conf. on Intelligent Robots & Systems (IROS '98)*, Victoria, BC, Canada, October 1998.

[4] Lichten, M. D., and S. Dubowsky, "State, shape, and parameter estimation of space objects from range images," in *Proc. IEEE Int. Conf. Robot. Autom.*, New Orleans, USA, 2004, pp. 2974-2979.

[5] Hillenbrand, U., and R. Lampariello, "Motion and parameter estimation of a free-floating space object from range data for motion prediction," in *Proc. iSAIRAS*, Munich, Germany, 2005.

[6] Aghili, F., "A prediction and motion-planning scheme for visually guided robotic capturing of free-floating tumbling objects with uncertain dynamics," *IEEE Tr. Robot. Autom.*, vol. 28, no. 3, pp. 634-649, Jun. 2012.

[7] Sheinfeld, D., and S. Rock, "Rigid body inertia estimation with applications to the capture of a tumbling satellite," in *Proc. 19th AAS/AIAA Spaceflight Mech. Meet.*, vol. 134, pp. 343-356, 2009.

[8] Meng, Q., J. Liang and O. Ma, "Estimate of all the inertial parameters of a free-floating object in space," in *AIAA Guid., Nav. Control Conf.*, Kissimmee, Florida, 2018, pp. 1606.

[9] Christidi-Loumpasefski, O.-O., and E. Papadopoulos, "Parameter identification of a space object in the pre-capture phase," in *Proc. Int. Symp. Artif. Intell. Robot. Autom. Space*, Madrid, Spain, 2018.

[10] Murotsu, Y., K. Senda, M. Ozaki, and S. Tsujio, "Parameter identification of unknown object handled by free-flying space robot," *AIAA J. Guid., Control, Dyn.*, vol. 17, no. 3, 1994, pp. 488-494.

[11] Lampariello, R. and G. Hirzinger, "Modeling and experimental design for the on-orbit inertial parameter identification of free-flying space robots," in *Proc. IDETC/CIE 2005 ASME 2005 Int. Des. Eng. Tech. Conf. Comp. Inf. Eng. Conf.*, Long Beach, CA, USA, 2005, pp. 1-10.

[12] Rackl, W., R. Lampariello, and A. Albu-Schaffer, "Parameter identification methods for free-floating space robots with direct torque sensing," in *IFAC Proc. Vol.*, vol. 46, no. 19, pp. 464-469, 2013.

[13] Nabavi-Chashmi, S.-Y., and S.-M.B. Malaek, "Inertial parameter identification using contact force information for an unknown object captured by a space manipulator," *Acta Astron.*, vol. 131, pp. 69-82, 2017.

[14] Ekal, M., and R. Ventura, "On inertial parameter estimation of a free-flying robot grasping an unknown object," in *Proc 5th Int. Conf. Con. Dec. Inf. Tech.*, Thessaloniki, Greece, 2018, pp. 815-821.

[15] Yoshida, K., and S. Abiko, "Inertia parameter identification for a free-flying space robot," *AIAA Guidance, Navigation, and Control Conference*, Monterey, CA, Aug. 2002.

[16] Ma, O. and H. Dang, "On-orbit identification of inertia properties of spacecraft using a robotic arm," *AIAA J. Guid., Control, Dyn.*, vol. 31, no. 6, pp. 1761-1771, 2008.

[17] Nguyen-Huynh, T.-C. and I. Sharf, "Adaptive reactionless motion and parameter identification in postcapture of space debris," *AIAA J. Guid., Control, Dyn.*, vol. 36, no. 2, pp. 404-414, 2013.

[18] Christidi-Loumpasefski, O.-O., K. Nanos, and E. Papadopoulos, "On parameter estimation of space manipulator systems using the angular momentum conservation," in *Proc. IEEE Int. Conf. Robot. Autom.*, Singapore, 2017, pp. 5453-5458.

[19] Xu, W., Z. Hu, Y. Zhang, Z., and B. Liang, "On-orbit identifying the inertia parameters of space robotic systems using simple equivalent dynamics," *Acta Astron.*, vol. 132, pp. 131-142, 2017.

[20] Papadopoulos, E., "On the nature of control algorithms for space manipulators," in *Proc. IEEE Int. Conf. Robot. Autom.*, Cincinnati, OH, pp. 1102-1108, 1990.

[21] Papadopoulos, E., "On the dynamics and control of space manipulators," Ph.D. dissertation, Dept. Mech. Eng., MIT, Cambridge, MA, 1990.

[22] Nanos, K. and E. Papadopoulos, "On the use of free-floating space robots in the presence of angular momentum," *Intell. Serv. Robot.*, vol. 4, no. 1, pp. 3-15, 2011.